Materials Advances

ROYAL SOCIETY OF CHEMISTRY

PAPER

View Article Online
View Journal | View Issue

Cite this: *Mater. Adv.*, 2025, **6**, 1067

Mussel-inspired novel coating with cariogenic biofilm inhibition and *in situ* remineralization properties for caries treatment

Jiaolong Wang, †[ab] Min Ge,†[ab] Huizhen Wang,†[ab] Haiyan Yao,[ab] Yunyun Deng[ab] and Junchao Wei *[ab]

Received 25th November 2024,
Accepted 23rd December 2024

DOI: 10.1039/d4ma01160k

rsc.li/materials-advances

Dental caries is a biofilm-mediated dynamic disease associated with imbalance in teeth mineralization. In this study, a facile and dual-functional hybrid polydopamine@proanthocyanidin (PDA@PC) coating was designed to inhibit cariogenic biofilm formation and remineralize demineralized dental hard tissues. PDA@PC exhibited excellent antibiofilm ability with a lower cariogenic bacterial biofilm biomass (0.15 ± 0.03 OD_{595nm}) than that (1.45 ± 0.16 OD_{595nm}) exhibited by the control group. In addition, a dense mineral layer was observed on the surface of demineralized enamel. The microhardness of etched enamel with the PDA@PC coating reached 329.28 ± 10.16 HV after incubation with artificial saliva, which was similar to the healthy enamel (368.5 ± 17.18 HV). Furthermore, the *in vivo* rat dental caries model showed that the PDA@PC coating effectively slowed down the progression of caries, with only superficial demineralization and low dental caries scores. The total score was 3–4 times lower than that of the control group. The successful construction of the dual-functional hybrid PDA@PC coating provides a novel approach for dental caries treatment.

1 Introduction

Dental caries is one of the most prevalent human diseases affecting more than 3.5 billion people worldwide.[1] The World Health Organization has identified dental caries as one of the primary diseases in humans to be prevented and controlled.[2] The continuous demineralization of dental hard tissues, caused by the acid production of bacteria in dental biofilms, leads to the development of caries.[3,4] Without timely intervention, dental caries may cause negative impacts such as pain, loss of teeth, sleeping difficulties, and even serious systemic inflammatory reactions.[5,6]

Current clinical approaches for caries treatment are invasive and implemented after the occurrence of tooth defects.[7] Moreover, the lack of antimicrobial properties in restoration materials and their failure to match the composition and mechanical properties of dental tissues result in secondary caries and fractures of prosthetics or teeth.[8–10] Meanwhile, traditional non-invasive treatments such as fluorides, mouthwashes, and dental floss reduce the cariogenic potential of biofilms by controlling dental plaque. However, these methods rely on patient compliance,[11] and household fluorides and mouthwashes have a mild therapeutic effect due to their low content of active ingredients. Since the main components of dental hard tissue are hydroxyapatite (HAP), many remineralization methods or products have been undertaken to restore defective enamel.[12–17] For example, fluorides form fluorapatite by substituting the hydroxyl groups in HAP and effectively reduce the incidence of dental caries.[18] However, this method is limited when residual seed crystallization is deficient.[19] Other products, such as calcium phosphate and bioglass, also merely form disordered mineral deposits, which are far from the dental structure.[20] Recently, biomimetic remineralization, inspired by the natural process of tooth mineralization, has provided numerous strategies for reconstructing dental hard tissues.[21] For example, self-assembled anionic peptides or amphiphilic peptides bioinspired by the structure and function of amelogenin have achieved effective HAP regeneration.[22,23] However, the peptide sequences are usually unavailable, and the complicated procedures limit their further clinical applications. Furthermore, these methods or products fail to take into account the risks of stubborn cariogenic biofilms in the demineralization lesions of caries, which tends to minimize their efficacy.[24,25] Therefore, combating cariogenic biofilms and regenerating defective dental hard tissues are essential for dental caries treatment.

[a] *School of Stomatology, Jiangxi Medical College, Nanchang University, Nanchang 330006, China. E-mail: weijunchao@ncu.edu.cn*
[b] *Jiangxi Province Key Laboratory of Oral Diseases & Jiangxi Province Clinical Research Center for Oral Diseases, Nanchang 330006, China*
† These authors contributed equally.

Proanthocyanidin (PC) is a plant-derived polyphenol known for its potent biological effects including antioxidative, anticancer, antibacterial, antibiofilm, and anti-inflammatory properties.[26] In the field of dentistry, the antibacterial and antibiofilm abilities of PC are particularly noteworthy. Previous studies have demonstrated that PC has the potential to effectively treat various oral infectious diseases such as periodontitis, dental caries, and oral mucositis.[27,28] In addition, the abundant phenolic hydroxyl groups in PC facilitate the deposition of mineral ions and promote HAP crystallization.[29,30] Based on these properties, PC is quite a good candidate for dental caries treatment. However, PC has insufficient adhesion and cannot be retained on the tooth surface for a long time when meeting the buffering effect of saliva in oral cavity.[31] To enhance adhesion, Li *et al.*, inspired by the peptide sequences of salivary acquired pellicle (SAP), developed a novel SAP-PC coating for dental caries treatment. The findings demonstrated that the SAP-PC coating can firmly adhere to the enamel surface. Furthermore, it effectively promoted mineralization and inhibited the formation of *Streptococcus mutans* (*S. mutans*) biofilm.[32,33] However, peptide sequences are not easily available, and the corresponding modification procedures are complicated. Therefore, more efficient strategies are required to assist the adhesion of PC to the tooth surface, and then exert antibiofilm and remineralization efficacy.

Inspired by the mussel-adhesion phenomenon in nature, polydopamine (PDA) coating can easily and firmly adhere to various types of material surfaces.[34] Owing to the abundant catechol/quinone groups of PDA, functional molecules or inorganic HAP crystals can anchor onto PDA by physical or chemical bonding.[35–37] Previous studies have also reported that PDA coating can effectively promote enamel remineralization and dentin tubule occlusion.[38–41] Therefore, due to its strong adhesion property, modifiability and mineralization ability, PDA can be used to construct a hybrid coating with PC for caries treatment.

In this study, a facile and dual-functional hybrid coating (PDA@PC coating) was constructed on the tooth surface for dental caries treatment. The coating was successfully prepared *via* the Michael addition and Schiff base reactions between PDA and PC (Scheme 1). First, enamel samples were simply immersed in a PC solution for 1 h, and then oxidative polymerization of dopamine resulted in an adhesive PDA@PC coating. Due to the improved adhesion, PC can effectively exert its antibiofilm property. Meanwhile, enamel surface-anchored phenolic hydroxyl groups and catecholamine moieties can induce calcium ion deposition in saliva. Both *in vitro* and *in vivo* experiments showed that the PDA@PC coating exhibited good performance in the inhibition of cariogenic bacterial biofilm formation and remineralization for dental caries treatment.

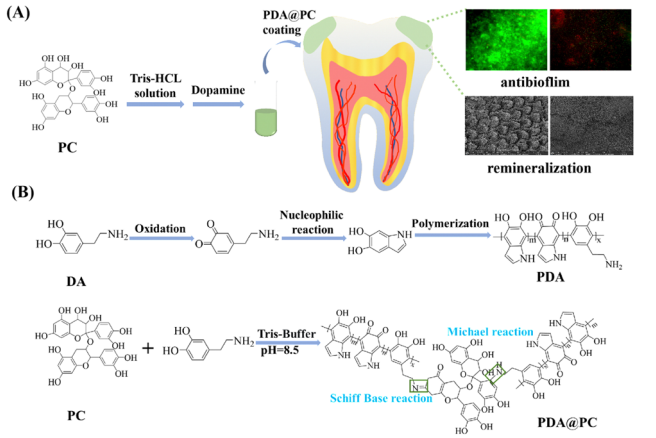

Scheme 1 Schematic of the PDA@PC coating with dual antibiofilm and remineralization functions (A). Schematic of PDA@PC synthesis (B).

2 Materials and methods

2.1 Materials

Dopamine hydrochloride (DA, 98%), tris(hydroxymethyl) aminomethane hydrochloride (Tris–HCl, 98%) and *N*-(2-hydroxyethyl)piperazine-*N*′-ethanesulfonic acid (HEPES) were purchased from Sigma-Aladdin Scientific Co., Ltd (Shanghai, China). Proanthocyanidins (PC, AR, >95%), calcium chloride ($CaCl_2$), potassium chloride (KCl) and potassium dihydrogen phosphate (KH_2PO_4) were purchased from Sinopharm Chemical Reagent Co., Ltd (Shanghai, China). Dulbecco's modified Eagle's medium (DMEM) was purchased from Solarbio Technology Co., Ltd (Beijing, China). Fetal bovine serum (FBS, 99%) was purchased from CellMax Cell Technology (Beijing) Co., Ltd. Acridine orange (AO) and ethidium bromide (EB) were purchased from Bestbio Biotechnology Co., Ltd (Shanghai, China). TRITC-labeled phalloidin (>90%) and 4′,6-diamidino-2-phenylindole (DAPI, >90%) were purchased from Maokang Biotechnology Co., Ltd (Shanghai, China). Triton X-100 was purchased from Thermo Fisher Scientific Co., Ltd, 4% paraformaldehyde was purchased from Sopo Biological Technology Co (Guangzhou, China). Brain heart infusion (BHI) broth was purchased from Qingdao Hope Bio-Technology Co., Ltd (China).

2.2 Preparation of demineralized enamel samples

Freshly extracted human third molars were collected with the approval of the Stomatological Hospital of Nanchang University. After removing the organic contaminants, teeth were immersed in 0.5% Chloramine T at 4 °C. The enamel samples were cut from the buccal, lingual, mesial, and proximal surfaces of each tooth, and then sequentially wet-polished with 600-, 800-, 1200-, and 2000-grit silicon carbide sandpapers. To simulate early caries lesions, the enamel samples were etched with 35% phosphoric acid gel for 1 min and then ultrasonicated for 10 min to remove the smear layer and stored in deionized water at 4 °C.

2.3 Preparation of PDA@PC coatings

First, 30 mg of PC was dissolved in 30 mL of Tris–HCL solution (10 mM, pH = 8.5). Demineralized enamel samples were immersed for 1 h. Then, 30 mg of dopamine hydrochloride was added and stirred for 0.5 h. Finally, the enamel samples

were rinsed with deionized water to remove the unattached molecules, resulting in PDA@PC-coated enamel. Moreover, other substrates such as cover slips, HAP discs, and molar crowns were also coated with PDA@PC by following the same procedures.

2.4 Evaluation of biocompatibility

An AO/EB cell assay kit and a TRITC-labeled phalloidin kit were used for evaluating the biocompatibility of PDA@PA coatings for mouse fibroblasts (L929 cells). Coverslips were used instead of enamels for better observation of biocompatibility. PDA@PC-coated coverslips were obtained by immersed coverslips in the PC solution for 1 h, followed by the same steps as the procedure depicted in Section 2.3. The blank coverslips and PDA@PC-coated coverslips were placed in 24-well plates, and then L929 cells were seeded onto the surface of coverslips at a density of 8×10^4 cells per well. After 48 h of coculture, these cells were processed for live/dead cell staining and cytoskeleton staining according to the specification. For live/dead cell staining, 50 μL of AO/EB solution was placed into each well and incubated for 5–10 min. As for cytoskeleton staining, L929 cells were fixed with 4% paraformaldehyde, permeabilized with 0.1%Triton X-100, blocked with bovine serum albumin, and then immunostained with TRITC-labeled phalloidin for F-actin filaments and 4′,6-diamidino-2-phenylindole (DAPI) for nucleus analysis in the darkness. Finally, the cells were observed by fluorescence microscopy (Leica, DMi8).

2.5 Antibiofilm experiments

2.5.1 Preparation of the cariogenic bacterial biofilm. In this study, *S. mutans* (ATCC 25175) was selected for bacterial cultivation and biofilm preparation. This bacterial strain was anaerobically incubated in a brain heart infusion (BHI) broth at 37 °C in an atmosphere containing 5% CO_2. Sterilized HAP discs and non-carious human molar crowns pretreated with or without the PDA@PC coating were used for antibiofilm experiments. First, HAP discs or molar crowns were placed in 48-well plates and cocultured with 800 μL of *S. mutans* (OD 600 = 0.3) under an anaerobic environment to form *S. mutans* biofilms. Then the BHI medium was refreshed every 12 h. After incubation for 48 h, these samples were gently washed 3 times with sterile PBS to remove unattached bacteria and transferred to new 48-well plates.

2.5.2 Live/dead staining of biofilms. After 48 h of incubation, the *S. mutans* biofilm on the HAP disc surface was stained with a live/dead BacLight Viability Kit. In detail, each HAP disc was stained with 10 μL mixture of NucGreen/EthD-III/0.85% NaCl for 15 min and then observed using a fluorescence microscope. Dead bacteria with defective cell membranes were stained with EthD-III to emit red fluorescence. At the same time, live bacteria were stained with NucGreen to emit green fluorescence.

2.5.3 Crystal violet staining of biofilms. Non-carious molar crowns were subjected to biofilm crystal violet staining. After 48 h, the *S. mutans* biofilm on each molar crown was fixed with 10% methanol for 30 min. Then, methanol was removed. Subsequently, 1% crystal violet dye was added to stain for 20 minutes. The crowns were then rinsed with sterile water to remove unbound dye and dried for further imaging. Next, 33% (w/v) acetic acid was added to dissolve the dye, followed by incubation in the darkness for 15 min. Finally, the absorbance was measured at 595 nm to quantify the biofilm biomass.

2.6 *In vitro* enamel remineralization

The demineralized enamel samples coated with or without PDA@PC coating were immersed in artificial saliva at 37 °C for *in vitro* remineralization experiments. The demineralized enamel samples without coating served as the control group. The artificial saliva (1.5 mM $CaCl_2$, 0.9 mM KH_2PO_4, 130 mM KCl, 20 mM HEPES, pH was adjusted to 7.0 with 1 mol L^{-1} KOH) was refreshed every 24 h. After 1, 4, 7, and 14 days, the enamel samples were washed and dried for subsequent examinations.

The surface morphology or mineral deposits of the enamel samples were observed by field emission scanning electron microscopy (FE-SEM, Apero C HiVac, USA) with a beam voltage of 5 kV. The wettability of the enamel surface was measured using a water contact angle tester (SL200 KS, USA). Besides, the surface microhardness was measured using a Vickers hardness tester (VH1202-01-0110, USA), with a diamond indenter under a 25-gf load for 10 s. Six sites of each sample were tested.

2.7 *In vivo* enamel remineralization

In vivo experiments were conducted with the approval of the Animal Experimental Ethics Committee of Nanchang University. The demineralized enamel samples with different thicknesses (approximately 2.5 mm and 1.2 mm, respectively) were prepared. Then these samples were pretreated by following the same procedure as the *in vitro* experiment. The demineralized enamel samples without coating served as the control group. Then twelve female SD rats (200–240 g) were anesthetized with pentobarbital sodium (70 mg kg^{-1}) and randomly divided into the control group and the PDA@PC group (n = 6). The enamel samples were disinfected with alcohol cotton, and then fixed in the oral cavity of rats using a 0.20 mm stainless steel ligature wire. Furthermore, a *S. mutans* suspension (200 μL, 1×10^8 CFU per mL) was inoculated on the enamel sample surface on the first 3 days, and the rats were fed with soft food containing 5% sucrose to establish a cariogenic environment. After 7 days, all the enamel samples were removed, rinsed with deionized water, and then investigated by FE-SEM and using a Vickers hardness tester.

2.8 *In vivo* dental caries model

Twelve 20-day-old female SD rats were used to establish the dental caries model for evaluating the therapeutic effect of PDA@PC coating. First, all rats were fed with the cariogenic Keyes 2000 Diet (Jiangsu Syony Bioengineering Co., Ltd, China) supplemented with 5% sucrose water. After infected with the *S. mutans* suspension for one week (10^8 CFU per mL, once a day), the rats were randomly divided into control and PDA@PC groups (n = 6). Next, 400 μL of sterile water or PDA@PC solution

(2 mg mL^{-1}) was locally smeared on the rat molars, the procedure lasted for 5 weeks (once a day during the first month, then once every two days for a week), and the rats were weighed weekly. Then, all rats were fed with a cariogenic diet for another 10 days without any local administration. On day 73, all the rats were sacrificed. Maxillary/mandibular jaws were isolated and stained with murexide solution (0.4%) for 12 h, and then hemisectioned along the mesiodistal sagittal plane. The progression of dental caries was evaluated using a stereoscopic microscope, following the Keyes caries scoring method.[42] In addition, the oral mucosa (tongue and buccal) and major organs were collected for Hematoxylin and eosin (H&E) staining to evaluate *in vivo* biocompatibility.

2.9 Statistical analysis

All the results are presented as mean ± standard deviation. The statistical difference between groups was examined using Student's *t*-test with significance accepted at $p < 0.05$.

3 Results and discussion

3.1 Biocompatibility of PDA@PC

Considering that cells tend to grow unevenly on the surface of enamel samples, coverslips were used for biocompatibility evaluation. First, live/dead staining of L929 cells was performed to evaluate the cytotoxicity. After 48 h coculture, the PDA@PC-coated coverslips had an equivalent cell density to that of the blank coverslips (Fig. 1A). There were large numbers of live cells labeled by green fluorescence and almost no red fluorescence-labeled dead cells, which suggested that PDA@PC can well support cell survival. Furthermore, the cell morphology of L929 cells was assessed by cytoskeleton staining (Fig. 1B). There was no obvious difference between the two groups. The cells showed active stretching, with regularly round and intact nuclei. These results indicated that PDA@PC has good biocompatibility to L929 cells.

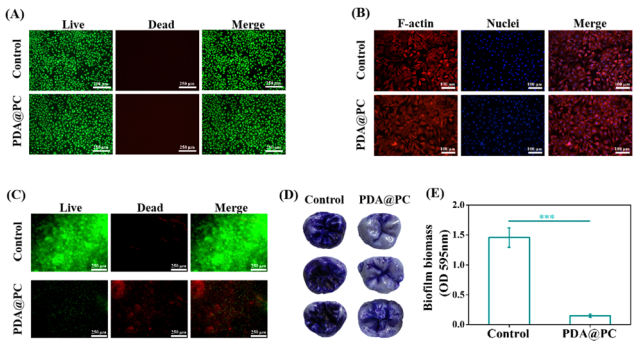

Fig. 1 Biocompatibility and antibiofilm activity of the PDA@PC coating: live/dead staining (A) and cytoskeleton staining (B) of L929 cells. Live/dead staining of biofilms (C). Crystal violet staining of biofilms (D) and corresponding biofilm biomass (E).

3.2 Antibiofilm activity of the PDA@PC coating

S. mutans is a well-known cariogenic bacterium which can adhere to the enamel surface and metabolize carbohydrates to produce organic acids, resulting in tooth demineralization and even the formation of dental caries. Therefore, *in vitro* experiments of *S. mutans* biofilms on the HAP discs or molar crowns that mimic the oral environment were established to investigate the antibiofilm effects of the PDA@PC coating.

The live/dead staining of *S. mutans* biofilm showed that the biofilm without PDA@PC pretreatment (the control group) maintained a relatively intact structure with dense bacteria dyed with green fluorescence (Fig. 1C). In contrast, for the PDA@PC group, the proportion of live bacteria significantly decreased, and the biofilm was broken and almost completely stained red (Fig. 1C). Then, the biofilms on the molar crowns were also observed and quantified by the crystal violet method. The biofilms of the control group were dense and dark purple, while biofilms in the PDA@PC group were slightly stained, and the pits and fissures of the molar crowns were still clear (Fig. 1D). The OD_{595nm} value of the corresponding biofilm biomass in the PDA@PC group was 0.15 ± 0.03, which was significantly lower than that of the control group (1.45 ± 0.16 OD_{595nm}) (Fig. 1E). Taken together, the PDA@PC coating can inhibit *S. mutans* biofilm formation and prevent teeth from suffering from dental caries. The antibiofilm mechanisms mainly include several aspects: (i) PC can interfere with the bacterial adhesion stage, thus reducing biofilm formation;[43] (ii) PC can bind with Ca^{2+} and Mg^{2+} on the membrane *via* chelation to destabilize the cell membrane, destroy the integrity of cell walls, and increase cell membrane permeability;[44] and (iii) PC can inhibit extracellular microbial enzymes and deprive microbial substrates needed for growth.[45,46]

3.3 *In vitro* enamel remineralization

In this study, non-caries human enamel samples were carefully polished and then etched for remineralization experiments. SEM images showed that the surface of normal enamel was relatively flat. In contrast, the elaborate structures of the prisms and interprisms became clear after acid etching (Fig. 2A). In addition, the water contact angle of normal enamel was 77.35 ± 5.07°; however, the value dramatically decreased to 15.43 ± 2.16° for the acid-etched enamel (Fig. 2B). This obvious change may be attributed to the rougher tooth surface caused by the dissolution of HAP minerals.

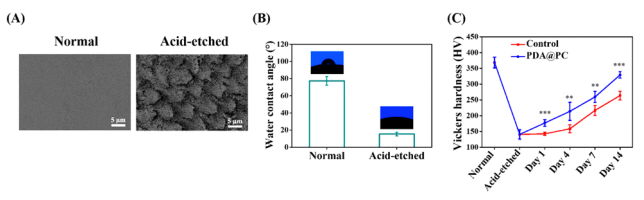

Fig. 2 SEM images (A) and water contact angles (B) of the enamel samples. (C) Surface Vickers hardness of normal enamel and acid-etched enamel samples after soaking in artificial saliva for 1 day, 4 days, 7 days and 14 days.

In vitro enamel remineralization experiment was carried out by immersing acid-etched enamel samples (the control group) or acid-etched enamel samples with PDA@PC coating (the PDA@PC group) in artificial saliva for 2 weeks. The typical "fish scale" morphology of etched enamel was still clearly visible after 7 days in the control group (Fig. 3). However, new mineral crystals began to grow in the interprismatic zones of PDA@PC group after only 4 days (Fig. 3). On day 14, a layer of crystalline minerals was formed on the enamel surface in the two groups. However, unlike the loose and disordered morphology in the control group, a dense mineral layer was observed on the surface of the acid-etched enamel. The regenerated mineral layer completely covered the enamel prisms (Fig. 3). It can be reasonable to assume that the mineral layer is somewhat similar to the rodless enamel in the outermost layer of enamel, which is aprismatic and highly mineralized and protects prismatic structures against acid and mechanical attacks.[12,47] Therefore, the recovery of mechanical properties is also critical for evaluating the mineralization efficiency. The Vickers hardness of normal enamel and etched enamel was 368.5 ± 17.18 HV and 140.96 ± 14.66 HV, respectively (Fig. 2C). With the extension of soaking time, the microhardness increased gradually. It was noteworthy that the microhardness recovery in the PDA@PC group was greater than that in the control group (**$P < 0.01$; ***$P < 0.001$). After 14 days, the microhardness of the PDA@PC group was 329.28 ± 10.16 HV, which was close to that of normal enamel. Combined with the observation of SEM, it suggested that the PDA@PC coating could restore the mechanical properties of enamel through efficient remineralization.

3.4 *In vivo* enamel remineralization

To further evaluate the remineralization effect of the PDA@PC coating *in vivo*, enamel samples were fixed to the upper jaw of rats for 7 days (Fig. 4A). First, we prepared enamel samples with a thickness of 1.2 mm to assess the resistance of the newly regenerated mineral layer to daily salivary flushing and food friction. The SEM images showed that the control group displayed a thin and loose mineral layer, while the PDA@PC group exhibited a dense regenerated mineral layer (Fig. 4B). Subsequently, to further verify the remineralization stability of the PDA@PC coating, we prepared enamel samples (2.5 mm thickness) thicker than the average crown height of SD rat molar teeth, so that the coating received friction from the soft tissue (Fig. 4C). After 7 days of oral incubation, the SEM images showed that the newly generated mineral layer on thick enamel samples in the control group (thick and etched enamel without PDA@PC coating) had low stiffness and was prone to fracture and microcracks. In contrast, the PDA@PC group (thick and etched enamel with PDA@PC coating) showed a dense and well-organized regenerated mineral layer with a homogeneous appearance even after being subjected to erosion by soft tissue friction (Fig. 4D). The SEM results were consistent with the Vickers hardness results of thick enamel samples. The Vickers hardness of the control group was only 232.4 ± 22 HV, while the Vickers hardness of the PDA@PC group increased significantly to 383.2 ± 19.8 HV, which was close to normal enamel (Fig. 4E). Thick enamel samples differed from thin enamel samples in that they were subjected not only to salivary scouring and food friction, but also to soft tissue chewing friction. Cracks and pits appeared on the surface of the thick enamel samples in the control group (Fig. 4D). Under the influence of soft tissue friction, the PDA@PC coatings still showed good remineralization, indicating that the induced regenerated minerals had good mechanical properties and the regenerated mineral layer was stable. In conclusion, the PDA@PC coating was effective at promoting enamel remineralization in a real oral environment, which is expected to be a promising candidate for clinical enamel repair.

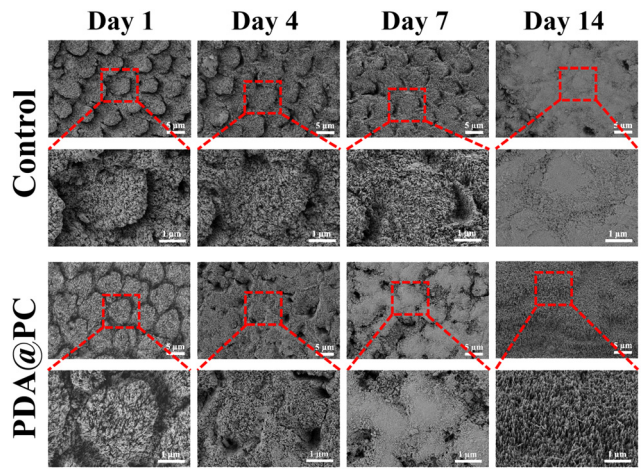

Fig. 3 SEM images of different enamel samples after soaking in artificial saliva for 1 day, 4 days, 7 days and 14 days.

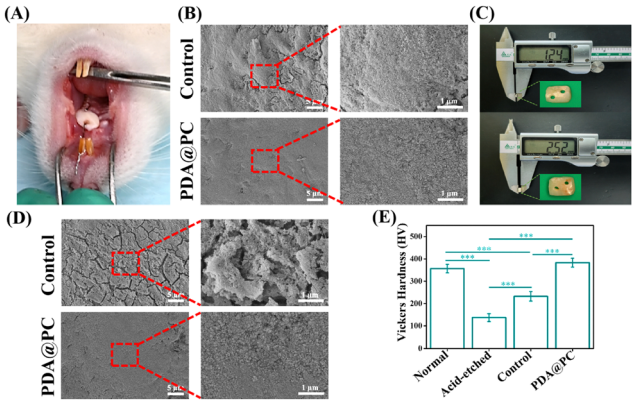

Fig. 4 Photograph of enamel fixed to the upper jaw of rat (A). SEM images of enamel after oral incubation (B). Photographs of enamel with different thicknesses (C). SEM images (D) and Vickers hardness (E) of thick enamel after oral incubation.

3.5 Dental caries treatment *in vivo*

The rodent caries model is widely accepted for evaluating the efficiency of dental caries treatment. Rat caries progressively from initial demineralization to moderate and extensive lesions are characterized by tooth structure damage and cavitation,

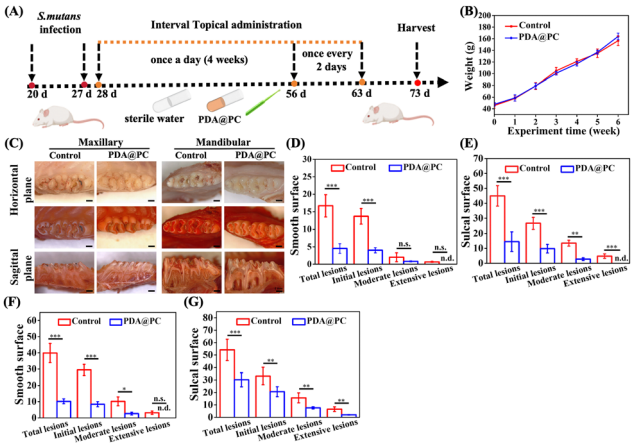

Fig. 5 Schematic diagram of *in vivo* experiment (A). Body weights of rats (B). Representative images of molars for different groups (C). Caries scores of smooth and sulcal surfaces in the maxillary arch (D) and (E) and the mandibular arch (F) and (G).

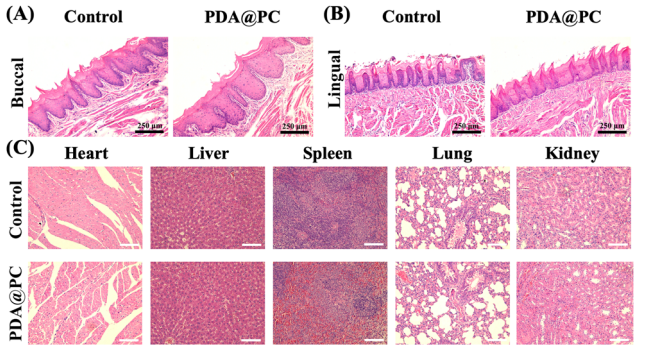

Fig. 6 H&E staining images of the buccal mucosa (A) and lingual mucosa (B) after PDA@PC coating. H&E staining images of the heart, liver, spleen, lung and kidney (C) after PDA@PC coating.

which is similar to caries development in humans.[48] Based on the excellent antibiofilm properties and remineralization performance, it is reasonable that the PDA@PC coating can perform well for *in vivo* dental caries treatment. The well-established rat caries and experimental procedures are shown in Fig. 5A. All rats survived until the experimental endpoint, and there was no significant difference in body weights between the two groups ($p > 0.05$, Fig. 5B). The enamel structure in the control group (without PDA@PC coating) was seriously damaged and carious lesions progressed to extensive dentin, resulting in obvious cavitation, while there was merely superficial demineralization without extensive dental damage in both the upper and lower dental arches in the PDA@PC group (Fig. 5C). Quantitative caries scoring analysis for the upper arch revealed that the control group had the most severe caries (Fig. 5D and E). For example, the total caries score of the sulcal surface reached 45 ± 6.8, and the moderate and extensive lesions accounted for a significant proportion. In contrast, PDA@PC greatly suppressed the initiation and progression of caries lesions on both smooth and sulcal surfaces ($P < 0.001$). Although the incidence of dental caries and the scores of initial and moderate lesion caries in the PDA@PC group increased slightly due to the poor efficiency of mandibular administration, they were still significantly lower than those in the control group (Fig. 5F and G). The probable reason for this phenomenon is that bacterial fluids and cariogenic foods are influenced by gravity and are more likely to accumulate in the mandibular arch. The above-mentioned results indicated that the PDA@PC coating was efficient in slowing down the progression of dental caries *in vivo*.

H&E staining images of the buccal and lingual mucosa are presented in Fig. 6A and B. No significant inflammation or other lesions were observed. Furthermore, the H&E staining was also employed to assess the potential toxicity to major organs (Fig. 6C). Similar to those in the control group, no organ abnormalities were found in the PDA@PC group. These histopathological results demonstrated the good biosafety of PDA@PC coating and further supported the application of PDA@PC in the oral environment for dental caries treatment.

4. Conclusions

In this study, we have successfully constructed a novel proanthocyanidin-grafted polydopamine coating *via* the Michael addition and Schiff base reactions on demineralized tooth enamel for dental caries treatment. Due to the improved adhesion inspired by the adhesion mechanism of mussels, PC can effectively exert its antibiofilm properties. Meanwhile, enamel surface-anchored phenolic hydroxyl groups and catecholamine moieties can induce calcium ion deposition in saliva. *In vitro* experiments showed that a PDA@PC coating effectively inhibited cariogenic biofilm formation, which are pivotal in dental caries. Moreover, it promoted the dense mineral layer formation, restoring the microhardness of the decayed enamel to that of healthy enamel. *In vivo*, PDA@PC coating thus effectively slowed down the progression of dental caries. Overall, this novel and dual-functional PDA@PC coating provides a convenient and promising strategy for dental caries treatment.

Author contributions

Jiaolong Wang, Min Ge and Huizhen Wang conducted the experiment and analyzed the data. Haiyan Yao and Yunyun Deng performed the processing of human teeth. Jiaolong Wang and Min Ge wrote, reviewed, and revised the manuscript. Junchao Wei and Jiaolong Wang designed the experiment and edited the manuscript.

Data availability

The data that support the findings of this study are available from the corresponding author upon request.

Conflicts of interest

There are no conflicts to declare.

Acknowledgements

This work was supported by the National Natural Science Foundation of China (52163016 and 82201078), Jiangxi Provincial program for the academic and technological leaders of main subjects (20213BCJL22051), and Jiangxi Provincial Natural Science Foundation (20224BAB216051).

Notes and references

1 N. Jain, U. Dutt, I. Radenkov and S. Jain, WHO's global oral health status report 2022: actions, discussion and implementation, *Oral Dis.*, 2024, **30**(2), 73–79, DOI: **10.1111/odi.14516**.

2 B. A. Dye, The Global Burden of Oral Disease: Research and Public Health Significance, *J. Dent. Res.*, 2017, **96**(4), 361–363, DOI: **10.1177/0022034517693567**.

3 N. B. Pitts, D. T. Zero, P. D. Marsh, K. Ekstrand, J. A. Weintraub, F. Ramos-Gomez, J. Tagami, S. Twetman, G. Tsakos and A. Ismail, Dental caries, *Nat. Rev. Dis. Primers*, 2017, **3**, 17030, DOI: **10.1038/nrdp.2017.30**.

4 N. Takahashi and B. Nyvad, Caries ecology revisited: microbial dynamics and the caries process, *Caries Res.*, 2008, **42**(6), 409–418, DOI: **10.1159/000159604**.

5 R. Hummel, N. A. E. Akveld, J. J. M. Bruers, W. J. M. van der Sanden, N. Su and G. J. M. G. van der Heijden, Caries Progression Rates Revisited: A Systematic Review, *J. Dent. Res.*, 2019, **98**(7), 746–754, DOI: **10.1177/0022034519847953**.

6 R. J. Schroth, J. Levi, E. Kliewer, J. Friel and M. E. K. Moffatt, Association between iron status, iron deficiency anaemia, and severe early childhood caries: a case-control study, *BMC Pediatr.*, 2013, **13**, 22, DOI: **10.1186/1471-2431-13-22**.

7 H. Desai, C. A. Stewart and Y. Finer, Minimally Invasive Therapies for the Management of Dental Caries-A Literature Review, *Dent. J.*, 2021, **9**(12), 147, DOI: **10.3390/dj9120147**.

8 J. L. Drummond, Degradation, fatigue, and failure of resin dental composite materials, *J. Dent. Res.*, 2008, **87**(8), 710–719, DOI: **10.1177/154405910808700802**.

9 A. F. Montagner, T. T. Maske, N. J. Opdam, J. J. de Soet, M. S. Cenci and M. C. Huysmans, Failed bonded interfaces submitted to microcosm biofilm caries development, *J. Dent.*, 2016, **52**, 63–69, DOI: **10.1016/j.jdent.2016.07.007**.

10 I. Nedeljkovic, J. De Munck, A. Vanloy, D. Declerck, P. Lambrechts, M. Peumans, W. Teughels, B. Van Meerbeek and K. L. Van Landuyt, Secondary caries: prevalence, characteristics, and approach, *Clin. Oral. Investig.*, 2020, **24**(2), 683–691, DOI: **10.1007/s00784-019-02894-0**.

11 N. B. Pitts, Are we ready to move from operative to non-operative/preventive treatment of dental caries in clinical practice?, *Caries Res.*, 2004, **38**(3), 294–304, DOI: **10.1159/000077769**.

12 B. Yeom, T. Sain, N. Lacevic, D. Bukharina, S. H. Cha, A. M. Waas, E. M. Arruda and N. A. Kotov, Abiotic tooth enamel, *Nature*, 2017, **543**(7643), 95–98, DOI: **10.1038/nature21410**.

13 E. A. Abou Neel, A. Aljabo, A. Strange, S. Ibrahim, M. Coathup, A. M. Young, L. Bozec and V. Mudera, Demineralization-remineralization dynamics in teeth and bone, *Int. J. Nanomed.*, 2016, **11**, 4743–4763, DOI: **10.2147/IJN.S107624**.

14 F. Clift, Artificial methods for the remineralization of hydroxyapatite in enamel, *Mater. Today Chem.*, 2021, **21**, 100498, DOI: **10.1016/j.mtchem.2021.100498**.

15 M. Chen, J. Yang, J. Li, K. Liang, L. He, Z. Lin, X. Chen, X. Ren and J. Li, Modulated regeneration of acid-etched human tooth enamel by a functionalized dendrimer that is an analog of amelogenin, *Acta Biomater.*, 2014, **10**(10), 4437–4446, DOI: **10.1016/j.actbio.2014.05.016**.

16 M. Schweikle, S. H. Bjørnøy, A. T. J. van Helvoort, H. J. Haugen, P. Sikorski and H. Tiainen, Stabilisation of amorphous calcium phosphate in polyethylene glycol hydrogels, *Acta Biomater.*, 2019, **90**, 132–145, DOI: **10.1016/j.actbio.2019.03.044**.

17 Z. Wang, Z. Zhou, J. Fan, L. Zhang, Z. Zhang, Z. Wu, Y. Shi, H. Zheng, Z. Zhang, R. Tang and B. Fu, Hydroxypropylmethylcellulose as a film and hydrogel carrier for ACP nanoprecursors to deliver biomimetic mineralization, *J. Nanobiotechnol.*, 2021, **19**(1), 385, DOI: **10.1186/s12951-021-01133-7**.

18 O. Y. Yu, M. L. Mei, I. S. Zhao, E. C. M. Lo and C. H. Chu, Effects of Fluoride on Two Chemical Models of Enamel Demineralization, *Materials*, 2017, **10**(11), 1245, DOI: **10.3390/ma10111245**.

19 L. L. Dai, M. L. Mei, C. H. Chu and E. C. M. Lo, Remineralizing effect of a new strontium-doped bioactive glass and fluoride on demineralized enamel and dentine, *J. Dent.*, 2021, **108**, 103633, DOI: **10.1016/j.jdent.2021.103633**.

20 A. A. Taha, M. P. Patel, R. G. Hill and P. S. Fleming, The effect of bioactive glasses on enamel remineralization: a systematic review, *J. Dent.*, 2017, **67**, 9–17, DOI: **10.1016/j.jdent.2017.09.007**.

21 B. Hu, Y. Pang, X. Yang, K. Xuan, X. Zhang and P. Yang, Advancements in dental hard tissue restorative materials and challenge of clinical translation, *Sci. China Mater.*, 2024, **67**(12), 3811–3832, DOI: **10.1007/s40843-024-3137-4**.

22 S. Dogan, H. Fong, D. T. Yucesoy, T. Cousin, C. Gresswell, S. Dag, G. Huang and M. Sarikaya, Biomimetic Tooth Repair: Amelogenin-Derived Peptide Enables in Vitro Remineralization of Human Enamel, *ACS Biomater. Sci. Eng.*, 2018, **4**(5), 1788–1796, DOI: **10.1021/acsbiomaterials.7b00959**.

23 Y. Zhou, Y. Zhou, L. Gao, C. Wu and J. Chang, Synthesis of artificial dental enamel by an elastin-like polypeptide assisted biomimetic approach, *J. Mater. Chem. B*, 2018, **6**(5), 844–853, DOI: **10.1039/c7tb02576a**.

24 M. A. S. Melo, S. F. F. Guedes, H. H. K. Xu and L. K. A. Rodrigues, Nanotechnology-based restorative materials for dental caries management, *Trends Biotechnol.*, 2013, **31**(8), 459–467, DOI: **10.1016/j.tibtech.2013.05.010**.

25 Y. Xu, Y. You, L. Yi, X. Wu, Y. Zhao, J. Yu, H. Liu, Y. Shen, J. Guo and C. Huang, Dental plaque-inspired versatile nanosystem for caries prevention and tooth restoration, *Bioact. Mater.*, 2023, **20**, 418–433, DOI: 10.1016/j.bioactmat.2022.06.010.

26 Q. An, X. Gong, L. Le, D. Zhu, D. Xiang, F. Geng, H. Zhu, L. Peng, L. Zou, G. Zhao and Y. Wan, Prospects for Proanthocyanidins from Grape Seed: Extraction Technologies and Diverse Bioactivity, *Food Rev. Int.*, 2023, **39**(1), 349–368, DOI: 10.1080/87559129.2021.1906699.

27 H. Chen, W. Wang, S. Yu, H. Wang, Z. Tian and S. Zhu, Procyanidins and Their Therapeutic Potential against Oral Diseases, *Molecules*, 2022, **27**(9), 2932, DOI: 10.3390/molecules27092932.

28 A. Furiga, A. Lonvaud-Funel, G. Dorignac and C. Badet, In vitro anti-bacterial and anti-adherence effects of natural polyphenolic compounds on oral bacteria, *J. Appl. Microbiol.*, 2008, **105**(5), 1470–1476, DOI: 10.1111/j.1365-2672.2008.03882.x.

29 M. Reis, B. Zhou, Y. Alania, A. A. Leme-Kraus, S. Jing, J. B. McAlpine, S. Chen, G. F. Pauli and A. K. Bedran-Russo, Unveiling structure-activity relationships of proanthocyanidins with dentin collagen, *Dent. Mater.*, 2021, **37**(11), 1633–1644, DOI: 10.1016/j.dental.2021.08.013.

30 Y. Zhang, Y. Huang, Y. Pang, Z. Zhu, Y. Zhang, Q. Liu, X. Zhang and Y. Liu, Modification of collagen with proanthocyanidins by mimicking the bridging role of glycosaminoglycans for dentine remineralization, *Mater. Des.*, 2021, **210**, 110067, DOI: 10.1016/j.matdes.2021.110067.

31 B. J. Teubl, B. Stojkovic, D. Docter, E. Pritz, G. Leitinger, I. Poberaj, R. Prassl, R. H. Stauber, E. Froehlich, J. Khinast and E. Roblegg, The effect of saliva on the fate of nanoparticles, *Clin. Oral. Investig.*, 2018, **22**(2), 929–940, DOI: 10.1007/s00784-017-2172-5.

32 S. Zhang, L. He, Y. Yang, B. Yang, Y. Liao, X. Xu, J. Li, X. Yang and J. Li, Effective in situ repair and bacteriostatic material of tooth enamel based on salivary acquired pellicle inspired oligomeric procyanidins, *Polym. Chem.*, 2016, **7**(44), 6761–6769, DOI: 10.1039/C6PY01362G.

33 X. Yang, B. Yang, L. He, R. Li, Y. Liao, S. Zhang, Y. Yang, X. Xu, D. Zhang, H. Tan, J. Li and J. Li, Bioinspired Peptide-Decorated Tannic Acid for in Situ Remineralization of Tooth Enamel: In Vitro and in Vivo Evaluation, *ACS Biomater. Sci. Eng.*, 2017, **3**(12), 3553–3562, DOI: 10.1021/acsbiomaterials.7b00623.

34 H. Lee, S. M. Dellatore, W. M. Miller and P. B. Messersmith, Mussel-inspired surface chemistry for multifunctional coatings, *Science*, 2007, **318**(5849), 426–430, DOI: 10.1126/science.1147241.

35 X. Xie, J. Tang, Y. Xing, Z. Wang, T. Ding, J. Zhang and K. Cai, Intervention of Polydopamine Assembly and Adhesion on Nanoscale Interfaces: State-of-the-Art Designs and Biomedical Applications, *Adv. Healthcare Mater.*, 2021, **10**(9), e2002138, DOI: 10.1002/adhm.202002138.

36 W. Cheng, X. Zeng, H. Chen, Z. Li, W. Zeng, L. Mei and Y. Zhao, Versatile Polydopamine Platforms: Synthesis and Promising Applications for Surface Modification and Advanced Nanomedicine, *ACS Nano*, 2019, **13**(8), 8537–8565, DOI: 10.1021/acsnano.9b04436.

37 J. Ryu, S. H. Ku, H. Lee and C. B. Park, Mussel-Inspired Polydopamine Coating as a Universal Route to Hydroxyapatite Crystallization, *Adv. Funct. Mater.*, 2010, **20**, 2132–2139, DOI: 10.1002/adfm.200902347.

38 W. Z. Qiu, H. C. Yang and Z. K. Xu, Dopamine-assisted co-deposition: an emerging and promising strategy for surface modification, *Adv. Colloid Interface Sci.*, 2018, **256**, 111–125, DOI: 10.1016/j.cis.2018.04.011.

39 Y. Z. Zhou, Y. Cao, W. Liu, C. H. Chu and Q. L. Li, Polydopamine-induced tooth remineralization, *ACS Appl. Mater. Interfaces*, 2012, **4**(12), 6901–6910, DOI: 10.1021/am302041b.

40 Y. Qu, T. Gu, Q. Du, C. Shao, J. Wang, B. Jin, Q. Kong, J. Sun, C. Chen, H. Pan, R. Tang and X. Gu, Polydopamine Promotes Dentin Remineralization via Interfacial Control, *ACS Biomater. Sci. Eng.*, 2020, **6**(6), 3327–3334, DOI: 10.1021/acsbiomaterials.0c00035.

41 Y. Li, L. Wu, Q. Wang, Q. Zhou, C. Cao, S. Zheng, Z. Zhou, H. Wong and Q. Li, Polydopamine-assisted co-deposition of polyacrylic acid inducing dentin biomimetic mineralization for tooth-like structure repair in vitro, *Mater. Today Chem.*, 2022, **24**, 10077, DOI: 10.1016/j.mtchem.2022.100775.

42 Y. Wang, Y. Zeng, Y. Wang, H. Li, S. Yu, W. Jiang, Y. Li and L. Zhang, Antimicrobial peptide GH12 targets Streptococcus mutans to arrest caries development in rats, *J. Oral. Microbiol.*, 2019, **11**(1), 1549921, DOI: 10.1080/20002297.2018.1549921.

43 M. C. Sánchez, H. Ribeiro-Vidal, B. Bartolomé, E. Figuero, M. V. Moreno-Arribas, M. Sanz and D. Herrera, New Evidences of Antibacterial Effects of Cranberry Against Periodontal Pathogens, *Foods*, 2020, **9**(2), 246, DOI: 10.3390/foods9020246.

44 A. Lacombe, V. C. H. Wu, S. Tyler and K. Edwards, Antimicrobial action of the American cranberry constituents; phenolics, anthocyanins, and organic acids, against Escherichia coli O157:H7, *Int. J. Food Microbiol.*, 2010, **139**(1–2), 102–107, DOI: 10.1016/j.ijfoodmicro.2010.01.035.

45 A. Smeriglio, D. Barreca, E. Bellocco and D. Trombetta, Proanthocyanidins and hydrolysable tannins: occurrence, dietary intake and pharmacological effects, *Br. J. Pharmacol.*, 2017, **174**(11), 1244–1262, DOI: 10.1111/bph.13630.

46 D. Kim, G. Hwang, Y. Liu, Y. Wang, A. P. Singh, N. Vorsa and H. Koo, Cranberry Flavonoids Modulate Cariogenic Properties of Mixed-Species Biofilm through Exopolysaccharides-Matrix Disruption, *PLoS One*, 2015, **10**(12), e0145844, DOI: 10.1371/journal.pone.0145844.

47 K. Mukherjee, Q. Ruan, S. Nutt, J. Tao, J. J. De Yoreo and J. Moradian-Oldak, Peptide-Based Bioinspired Approach to Regrowing Multilayered Aprismatic Enamel, *ACS Omega*, 2018, **3**(3), 2546–2557, DOI: 10.1021/acsomega.7b02004.

48 P. H. Keyes, Dental caries in the molar teeth of rats. II. A method for diagnosing and scoring several types of lesions simultaneously, *J. Dent. Res.*, 1958, **37**(6), 1088–1099, DOI: 10.1177/00220345803700609012.